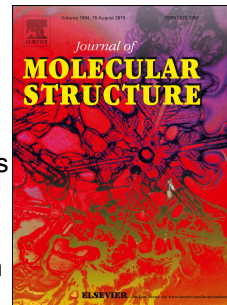


Accepted Manuscript

X-ray crystallographic analysis and DFT calculations of three 'propylene linker' dimers linked by one polystep reaction

Yan Shi, Xue-Jie Tan, Dian-Xiang Xing, Qi-Cheng Sui, Bin Liu, Wen-Quan Feng, Yun Liu



PII: S0022-2860(17)30138-2

DOI: [10.1016/j.molstruc.2017.02.006](https://doi.org/10.1016/j.molstruc.2017.02.006)

Reference: MOLSTR 23400

To appear in: *Journal of Molecular Structure*

Received Date: 29 November 2016

Revised Date: 28 January 2017

Accepted Date: 1 February 2017

Please cite this article as: Y. Shi, X.-J. Tan, D.-X. Xing, Q.-C. Sui, B. Liu, W.-Q. Feng, Y. Liu, X-ray crystallographic analysis and DFT calculations of three 'propylene linker' dimers linked by one polystep reaction, *Journal of Molecular Structure* (2017), doi: 10.1016/j.molstruc.2017.02.006.

This is a PDF file of an unedited manuscript that has been accepted for publication. As a service to our customers we are providing this early version of the manuscript. The manuscript will undergo copyediting, typesetting, and review of the resulting proof before it is published in its final form. Please note that during the production process errors may be discovered which could affect the content, and all legal disclaimers that apply to the journal pertain.

X-ray crystallographic analysis and DFT calculations of three ‘propylene linker’ dimers linked by one polystep reaction

Yan Shi ^a, Xue-Jie Tan ^{a*}, Dian-Xiang Xing ^a, Qi-Cheng Sui ^a, Bin Liu ^a, Wen-Quan Feng ^a, Yun Liu ^a

^a School of Chemistry and Pharmaceutical Engineering, Qilu University of Technology, Jinan, Shandong Province, 250353, P. R. China.

Abstract

In this manuscript, we report the synthesis, NMR and single-crystal structures of three propylene linking dimers related with the hydrolytic degradation of one 5,6-dehydronorcantharimide dimer. Special attention was paid to the conformation of propylene linkers in order to understand their changes in the reaction. Statistical analysis of CSD database revealed that a-a, g-a and g-g conformations may have similar stability in most cases and various complicated unpredictable non-covalent interactions may play important role in the formation of final rotamers.

In order to reproduce all stable conformations and the energy barriers separating them, full range two-dimensional fully relaxed potential-energy surfaces (PES) scans of six ‘propylene linker’ dimers were calculated starting from the most stable crystal structures. The PES were scanned along both bridge C-C single bond torsional angles (denoted as θ_1 and θ_2), while all other internal coordinates were optimized at the DFT/B3LYP/3-21G* level in gas phase. Then all energy minima were re-optimized again at the DFT/B3LYP/6-311+G(d,p) level both in gas and ethanol solutions in order to evaluate the really stable rotamers. At last, 1D or 2D relaxed PES scans were performed between local stable rotamers to get reliable energy barriers. This method represents a less time-consuming and more reliable approach to the determination of conformational stability of propanediyl bridging chains.

The combination of experimental, statistical and theoretical results shows that the observed conformation is jointly determined by the energy levels of the minima, energy barriers separating them, non-covalent interactions and somewhat randomness.

1. Introduction

The dimer structure is ubiquitous in natural products and dimeric molecules would be expected to show enhanced biological activity relative to their corresponding monomeric counterparts. [1] Dimeric compounds have been synthesized and studied for the treatment of cancer, HIV, Alzheimer, malaria and various parasitic diseases. [2] Meanwhile, tethering two functional headgroups together with a polymethylene chain (a short alkane linker) is being successfully used in designing functional materials following the concept of crystal engineering. [3] Among these alkane linking groups, propanediyl bridging chain is of particular interest on the point that these alkyl spacers should generally be long enough to result in significant conformational changes and on the other hand they should not be overly lengthy to make the synthesis and characterization difficult (probably due to the entropy effect). [4] Another point lies in the odd number of $-(CH_2)-$ groups, which may differ significantly from those of their even analogues. [5] Even more interesting was the fact that the spacer fragments provided by $-(CH_2)_3-$ units often meet better spatial demands in biomimetic / coordination / catalytic Chemistry than other polymethylene linkers. [6] As a result, the use of the ‘trimethylene linker’ has been increased in many studies. [7] However, systematic examinations on the conformational geometry and stability of the propylene linker are scarce. Gellman, S. H. and coworkers carried out conformational searches for 1,3-diphenylpropane and proved that all of the resulting local minima with the phenyl groups near one

^a Corresponding author. E-mail: tanxuejie@163.com, Tel.: +86 531 89631208; fax: +86 531 89631207.

another had the rings roughly parallel (fully stacked or offset) instead of perpendicular phenyl juxtapositions. [7(b)] Obviously, they mainly focused on the aromatic stacking interactions induced by aromatic-aromatic geometries instead of the conformations of the propylene linker itself. So the bridging chains are not well understood and there is an urgent need for more systematic models without too much bias for certain conformations, in which the type of dimer shapes can adjust or control the non-covalent interactions, such as hydrogen bonds, anion... π , [8] cation... π , π ... π interactions and X-H... π (X = C, N, O) interactions, or even intramolecular C-H ^{δ^+} ... δ^+ H-C interactions. [9] In other words, advances in rational supramolecular design will require a detailed understanding of the conformations of the propylene linker itself instead of too much kinds of weak interactions, which may be influenced by tons of factors, for example, terminal groups, substituents effect, steric effects, electrostatic effects, position of the 'propylene linker'. [3(e)] Is there any probability to realize the prediction and rational design of particular conformations regardless of all these complicated weak interaction? The combination of experimental, statistical, and theoretical studies will provide a new way in this area.

The rapid progress of computational hardware opens the possibility to apply more demanding computational methods, especially density functional theoretical (DFT) methods, to probe the conformational preferences of flexible molecules. [10] DFT methods are dominant over other computational techniques because it can yield excellent geometry and vibrational energies for compounds containing first and second row atoms. [11] On the other hand, hybrid functionals, [12] such as B3LYP, [13] yield good atomization energies [12,14] as well as good geometries and frequencies.

In view of these fascinating aspects of conformational geometry and diversity of the propylene linker presented above, we herein synthesized a series of three dimers in which different types of terminal groups are bridged by the same C₃ aliphatic chain and investigated their conformations in crystal state. On the base of our crystal structures and other similar crystal structures derived from CSD database, [15] potential energy surface (PES) scans were performed to reproduce the most stable conformations and the energy barriers separating different kinds of stable rotamers. We hope that the combined experimental and theoretical study may become a powerful tool in probing the conformational preferences of flexible molecules.

2. Experimental

2.1. Materials and measurements

All chemicals were purchased from Aladdin-reagent Chemicals and were used without further purification. Elemental (C, H, N) analyses were carried out with a Perkin-Elmer 2400 microanalyzer. ¹H NMR spectra were run on a Bruker Avance 400 MHz instruments. The chemical shifts are reported in parts per million (ppm) relative to tetramethylsilane, SiMe₄ ($\delta = 0$ ppm), referenced to the chemical shifts of residual solvent peak [deuterated dimethyl sulfoxide (DMSO-d₆)]. Melting points were determined on a WRS-2A electrothermal digital melting point apparatus (Shanghai precision & scientific instrument Co., Ltd, China).

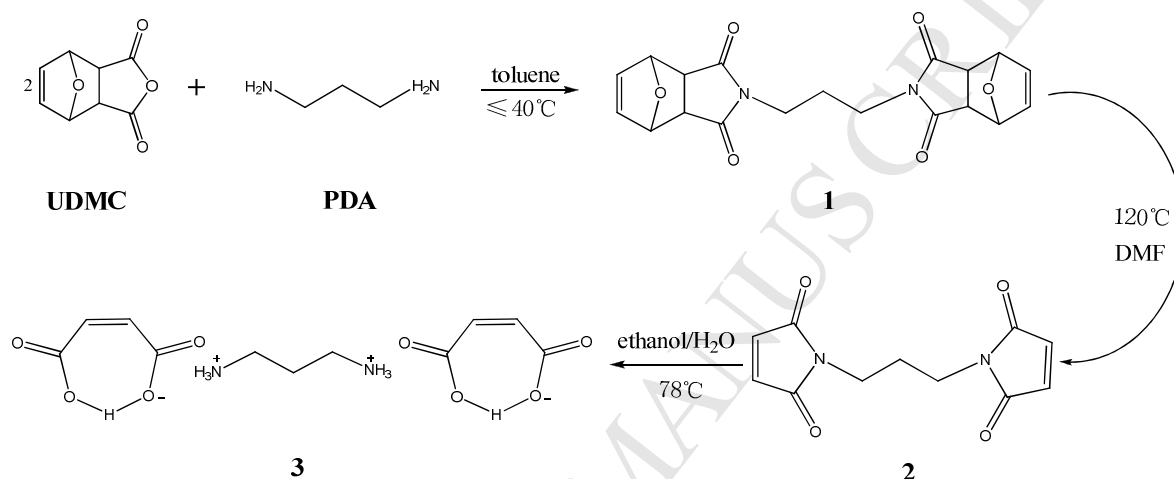
2.2. Synthesis and crystallization

Synthesis of unsaturated analogue of demethyl-cantharidin (UDMC) follows methods in the literature. [16] 0.833mL (0.01mol) propanediamine (PDA) was added to 50mL anhydrous toluene solution of 3.32g (0.02mol) UDMC and stirred vigorously for 24h. The solution became slightly yellow and pale yellow flocculent precipitate was obtained, which on re-crystallization from acetonitrile gave colorless crystals suitable for X-ray analysis in around 10% yield (dimer 1).

3.70g dimer **1** (0.01mol) was solved in 20 ml DMF and then heated over 120°C for 12 h, employing a reverse Diels-Alder reaction. The solvent was evaporated under reduced pressure to afford crude dimer **2**, which was re-crystallized in acetonitrile and colorless block crystals can be obtained in around 60% yield (1.40g).

A solution of dimer **2** (1.40g) in 30 mL ethanol/H₂O was refluxed for 24 h. The solvent was evaporated under reduced pressure to yield white residue. The residue was re-crystallized in water and colorless crystal (dimer **3**) can be obtained. The yield is about 70%. **3-1** and **3-2** were obtained in two different repetition experiments.

The general reactions are shown in **Scheme 1**:



Scheme 1. The reaction sequence in this paper. Systematic names for three products: **1**, 3,3'-(1,3-propanediyl)bis[3a,4,7,7a-tetrahydro-4,7-epoxy-1,3-bishydroisoindole-1,3-dione]; **2**, N,N'-propylenedimaleimide; **3**, propane-1,3-diammonium monohydrate bis(hydrogen maleate), **3-1** [or propane-1,3-diammonium bis(hydrogen maleate), **3-2**].

The physico-chemical characterization results are listed below (NMR spectra are shown in **Figs. S1-S6**. All "S" numbered tables and figures are in Supporting Information):

1 Elemental analysis: found (calc. for C₁₉H₁₈N₂O₆): C, 61.71 (61.62%); H, 4.96 (4.90%); N, 7.62 (7.56%); HRMS (ESI): *m/z* calcd for C₁₉H₁₈N₂O₆+H⁺: 371.1243 [*M*+H⁺]; found: 371.1237; M.p.149.1-150.1°C, ¹H NMR (DMSO): δ (ppm) 6.531(s, 4H, olefinic protons), 5.108(s, 4H, methine protons linked to bridge O, O-CH), 3.310(t, J=7.6Hz, 4H, methylene protons linked to imide N, N-CH₂-), 2.899(s,4H, methine protons, -CH-), 1.618(m, J=7.6Hz,2H, methylene protons, -CH₂-). ¹³C NMR (DMSO): δ (ppm) 176.275(carbonyl carbons), 136.397(olefinic carbons), 80.287(methine carbons linked to bridge O, O-CH-), 47.087(methine carbons, -CH-), 35.593(methylene carbons linked to imide N, N-CH₂-), 25.260(methylene carbons, -CH₂-). FT-TR(cm⁻¹,KBr): 3094(m, ν C=C-H), 3075(m, ν C=C-H), 3040(m, ν C=C-H), 3017(m, ν C=C-H), 2986(m, ν C-H), 2951(m, ν C-H), 1769(vs, ν C=O), 1717(vs, ν C=O), 1400(vs, ν C-N), 1169(vs, ν C-O-C); UV/Vis (CH₃CN) $\lambda_{\text{max}}/\text{nm}$ ($\epsilon/\text{L}\cdot\text{mol}^{-1}\cdot\text{cm}^{-1}$): 209.0(2.5 \times 10⁵).

2 Elemental analysis: found (calc. for C₁₁H₁₀N₂O₄): C, 56.61 (56.41%); H, 4.19 (4.30%); N, 12.26 (11.96%); M.p.169.5 -169.9°C (slightly different from literature [**17**] 172-174°C). ¹H NMR (CDCl₃): δ (ppm) 6.704(s, 4H, olefinic protons), 3.536 (t, J=7.2Hz, 4H, methylene protons linked to imide N, -N-CH₂-), 1.935 (m, J=7.2Hz, 2H, methylene protons, -CH₂-). ¹³C NMR (CDCl₃): δ (ppm) 170.583(carbonyl carbons), 134.224(olefinic carbons), 35.400(methylene carbons linked to imide N,

N-CH₂-), 27.436(methylene carbon, -CH₂-).

3 (in fact **3-2**) Elemental analysis: found (calc. for C₁₁H₁₈N₂O₈): C, 43.07 (43.14%); H, 6.16 (5.92%); N, 9.06 (9.15%); M.p.178.2-179.9°C. ¹H NMR (DMSO): δ (ppm) 7.728(s, 6H, -NH₃⁺), 6.018 (s, 4H, olefinic protons in maleic acid), 3.071(t, J=7.2Hz, 4H, methylene protons linked to -NH₃⁺, -N-CH₂-), 1.628 (m, J=7.2Hz, 2H, methylene protons, -CH₂-). ¹³C NMR (DMSO): δ (ppm) 167.117(carbonyl carbons), 135.128(olefinic carbons), 38.607(methylene carbons linked to -NH₃⁺, N-CH₂-), 25.314(methylene carbon, -CH₂-).

2.3 X-Ray Crystallographic Analysis

The X-ray diffraction measurements were made on a Bruker APEX II CCD area detector diffractometer at 293/298K for compounds **1** to **3** (Mo K α radiation, graphite monochromator, λ = 0.71073 Å). The structures were solved by SHELXL-97. The absorption correction was done using the SADABS program. [18] Software packages APEX II (data collection), SAINT (cell refinement and data reduction), SHELXTL (data reduction, molecular graphics and publication material), DIAMOND (simplifying crystal packing diagram) were also used. [19-21] All non-hydrogen atoms were refined with anisotropic displacement parameters. **3** has two crystal structures, **3-1** and **3-2**, the former has one water molecule and the latter has none. In **3-2**, some hydrogen atoms were added to the structure model on calculated positions but in the rest three crystal structures, the positions of all hydrogen atoms (except H5 and H6 in **1**) were experimentally determined in electron density maps and refined without any constraints. Crystal data, data collection and structure refinement details are summarized in **Table 1**.

Table 1 Crystallographic data and structure refinements summary for three products.

Compounds	1	2	3-1	3-2
Chemical formula	C ₁₉ H ₁₈ N ₂ O ₆	C ₁₁ H ₁₀ N ₂ O ₄	3(C ₃ H ₁₂ N ₂) ²⁺ , 6(C ₄ H ₃ O ₄) ⁻ , H ₂ O	(C ₃ H ₁₂ N ₂) ²⁺ ·2(C ₄ H ₃ O ₄) ⁻
<i>Mr</i>	370.35	234.21	936.84	306.27
Crystal habit	block/colorless	block/colorless	block/colorless	block/colorless
Crystal system	monoclinic	monoclinic	monoclinic	monoclinic
Space group	<i>C2/c</i>	<i>C2/c</i>	<i>P2₁/c</i>	<i>Cc</i>
<i>a</i> /Å	21.61 (2),	19.395 (7)	14.7571 (8)	9.893 (5)
<i>b</i> /Å	6.961 (7)	6.714 (2)	35.9464 (16)	35.521 (19)
<i>c</i> /Å	13.351 (17)	9.132 (3)	8.2126 (5)	8.066 (4)
α /°	90.00	90.00	90.00	90.00
β /°	123.58 (3)	116.930 (4)	97.036 (6)	98.891 (8)
γ /°	90.00	90.00	90.00	90.00
<i>V</i> /Å ³	1673 (3)	1060.1 (6)	4323.7(4)	2800(2)
<i>Z</i>	4	4	4	8
<i>D</i> calc. /g·cm ⁻³	1.470	1.467	1.439	1.453
μ /mm ⁻¹	0.111	0.114	0.124	0.125
<i>T</i> /K	298	293	293	293
<i>F</i> (000)	776	488	1984	1296
<i>R</i> int	0.1152	0.058	0.045	0.043
<i>R</i> ₁ [<i>I</i> >2 σ (<i>I</i>)]	0.0736	0.0509	0.0570	0.0623
<i>wR</i> ₂ /reflections	0.1654/1463	0.1133/1035	0.1552/6317	0.1635/4050
<i>S</i>	1.129	1.102	1.035	0.916

2.4 Computational Study

In this work, density functional theory Becke3LYP calculations [12, 22] are used to map out the potential energy surfaces (PES) of these flexible dimers in order to confirm the geometries, energies, number of local conformational minima, the global minimum structure and barrier heights separating different kinds of conformations. In these scans, both of the dihedral angles (θ_1 and θ_2 , **scheme 2**) were scanned over their full range using an interval of 10° between points. Full geometry optimizations along all other coordinates were carried out. 1,369 point calculations were completed for every dimer. The initial geometries in these scans were first extracted from their single-crystal X-ray results and then optimized by employing DFT B3LYP/6-31+G* calculations. [23] These scans were carried out with the 3-21G* basis set because the relaxed scan method is too expensive on the time scale for large molecular dimers.

In order to determine the reliability of 3-21G* basis set, preliminary PES scans were carried out for **2** and **3** with 3-21G* and 6-31+G* basis sets respectively. These results are listed in **Fig. S8** (for **2** in 3-21G*), **Fig. S9** (for **2** in 6-31+G*), **Fig. S10** (for **3** in 3-21G*) and **Fig. S11** (for **3** in 6-31+G*) as comparison. Relative energies and dihedral angles (θ_1 and θ_2) of every minimum are listed in **Tables S13-S16**, respectively. It can be seen that they are similar in map shape (mainly including the numbers, sites, relative energies and energy barriers of local conformational minima). For example, there are 17 minima in **Fig. S8**, 12 minima in **Fig. S9**, both 14 minima in **Fig. S10** and **S11**. The highest energy gap between local minima is 13.02 kJ/mol in **Fig. S8**, but 3.24 kJ/mol in **Fig. S9** (much different in this case). The highest energy gap between local minima is 29.91 kJ/mol in **Fig. S10**, and 30.33 kJ/mol in **Fig. S11** (nearly the same in this case). The highest energy barrier is around 65 kJ/mol in **Fig. S8** and **S9**. This value is around 131 kJ/mol in **Fig. S10** and **S11**. Considering that all minima will be re-optimized with more sophisticated basis functions, all full range relaxed PES scans were computed by using the basis set 3-21G*.

It's worthy to be noted that the minima on the PES map don't correspond precisely to the local stable conformation, since these scans were carried out at specific values of dihedrals (θ_1 and θ_2 are fixed and all other structural variables were subjected to optimization). So all local conformational minima were fully optimized again with the 6-311+G(d,p) level both in gas and ethanol phases (using conductor-like polarizable continuum model (CPCM) [24]) in order to get the most stable conformations and most reliable energy barriers. The comparison of the PES scan results and all re-optimized local minima demonstrate which one is really the local/global minimum structures. Then relaxed one-dimensional or two-dimensional PES scans between two stable conformers were performed in 6-311+G(d,p) basis set to get the energy barriers. Such a barrier height, although somewhat underestimated with 10° step size, is indicative of the propensity of particular conformers.

All calculations were carried out using the Gaussian03 program package [25] on a Sunway BlueLight MPP supercomputer housed at the National Supercomputer Center in Jinan, China.

3. Results and Discussion

3.1 Single-crystal X-ray crystallography

3.1.1. Crystal structure of **1**

As an unsaturated norcantharimide (UNCI) dimer, **1** has been reported before, [26] but no detailed structure information has been described. Monomeric and packing structures of **1** are depicted in **Fig. 1**. As can be seen from the figure, the polycyclic imide skeleton has the *exo*-conformation, which is more stable than the *endo*- structure and inevitably becomes the overwhelmingly major products under thermodynamic control. [16(c), 27] As for the $-\text{CH}_2-\text{CH}_2-\text{CH}_2-$ linker, **1** prefers gauche-gauche mode

(abbreviated as g-g), which makes **1** twist and this mode may confer chirality to the dimer. The structure adopts C_2 point-group symmetry. Since the asymmetric unit contains only one half-molecule, and the C_2 axis is just parallel to the crystal b axis through C10 atom, so the two halves are really identical.

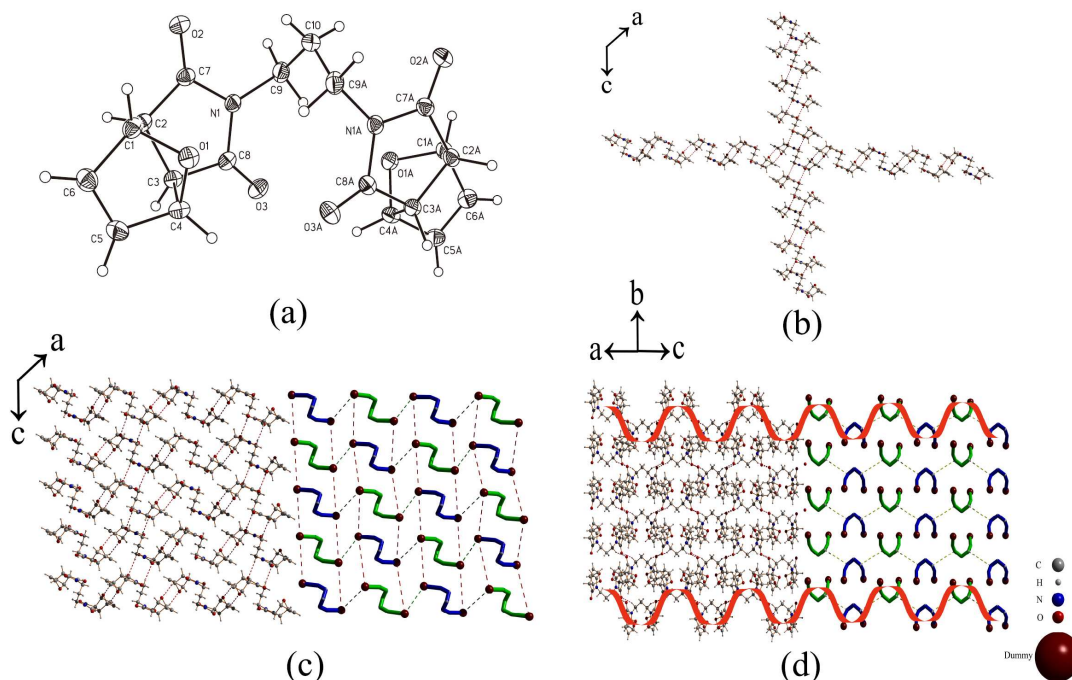


Fig. 1. (a) Atom numbered molecular structure of **1** with displacement ellipsoids for non-H atoms drawn at the 30% probability level at 298 K. “A” represents the symmetry code of “ $2-x, y, 0.5-z$ ”; (b) Two types of 1D chains of **1** formed through two kinds of intermolecular C–H...O H-bonds (shown red dotted lines), view along the b axis. The perpendicular chain extends along the c axis and the horizontal one extends along the $[-53\ 0\ -2]$ direction. (c) 2D structure formed by intermolecular C–H...O H-bonds, view along the b axis. The right half is illustrated by the simplified dimers, showing the supramolecular grid-like architecture. The simplified dimers are shown in different colors (blue and green) to emphasize their different orientations (same in the following figures). (d) Projection of the crystal structure on the plane $(1\ 0\ 1)$, purposing to show the arrangement of repeated layers extending perpendicular to the b axis.

In the packing structure of **1**, no valuable π - π stacking interactions can be found and the dominant force is hydrogen bonding. The geometries of hydrogen bonds are listed in **Table S1**. As can be seen, there are two kinds of intermolecular C–H...O hydrogen bonds in **1**, one involves carbonyl O ($C9-H9A...O2^{(-x+2, -y+1, -z)}$) and another involves bridge O ($C1-H1...O1^{(-x+3/2, -y+1/2, -z)}$). Each one of the two interactions link **1** into one kind of 1D chains with different orientations. The former chains orient along the c axis and the latter along the $[-53\ 0\ -2]$ direction (**Fig. 1b**). Then the two kinds of chains weave with each other leading to the formation of 2D tapes with the rhombic meshes parallel to the crystallographic ac plane (**Fig. 1c**). All dimers can be classified into two kinds of conformations, *i.e.* the two helical stereoisomers: the right-handed single helicate (P, in blue color) and the left-handed single helicate (M, in green color) (**Fig. 1c**). So, although every dimer unit is chiral, the presence of dimer units with opposite chirality makes the crystal achiral. As for the stacking geometries, the 2D layer framework is more like undulating tapes (**Fig. 1d**) due to the up and down points of adjacent helicates. Packing of these layers in the crystal is stabilized only by van der Waals forces.

3. 1. 2. Crystal structure of 2

Compound **2** was first synthesized in 1970 and its spectra and physical data have been reported several times [17, 26(b), 28], however its single-crystal structure has not been unambiguously determined till now.

Dimer **2** is not as complicated as **1** is in the point of headgroups. But they have very similar molecule and crystal structures. For example, they both adopt C_2 point-group symmetry and both have a C_2 axis just parallel to the crystal b axis through the central C atom (C10 and C6). They both crystallize in $C2/c$ space group, both contain one half-molecule in the asymmetric units and both have four formula units in the unit cell ($Z=4$). Even their unit cell parameters are similar (Table 1) except that **2** is somewhat smaller than **1**. As for the propanediyl bridging chain, they are also similar. The bond lengths of N-C are 1.465(4) and 1.4603(18) Å, C-C 1.515(5) and 1.5173(19) Å for **1** and **2**, respectively. Bond angles of N-C-C are 112.8(3) ° and 114.30(11) °, C-C-C 115.1(5) ° and 116.38 (17) °, respectively. Dihedral angles of N-C-C-C are 61.167(418) ° and 54.702 °, respectively. Obviously, dimer **2** maintains the same g-g conformation as that in dimer **1**.

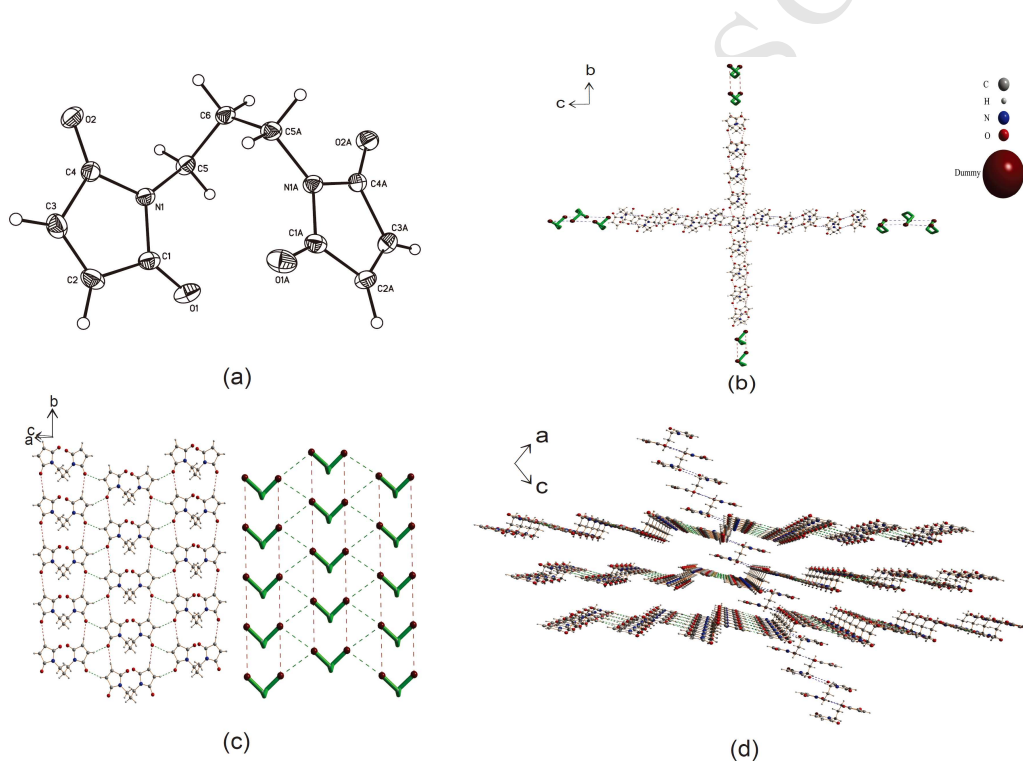


Fig. 2. (a) Atom numbered molecular structure of **2** with displacement ellipsoids for non-H atoms drawn at the 30% probability level at 293 K. Symmetry code of A: $-x, y, 0.5-z$. (b) Two kinds of 1D chains of **2** formed through two kinds of intermolecular C-H...O H-bonds, view along the a axis. C2-H1...O2 ($x, y+1, z$) (shown with red dotted lines) connect the dimer into a chain extends along the b axis; C5-H4...O1 ($-x, -y+1, -z$) (shown with blue dotted lines) connect the dimer into another chain extends along the c axis. Some dimers at the end of both chains are illustrated by the simplified structures, *i.e.* imide ring except N is simplified by its center gravity (red balls at each end of the chains) and all H atoms have been omitted for clarity. (c) Two-dimensional structure formed by the third kind of intermolecular H-bonds, C3-H2...O2 ($-x+0.5, y+0.5, -z+1.5$) (shown with green dotted lines), view perpendicular to the spreading plane, *i.e.* the crystallographic (2 0 -1) plane. The second H-bond mentioned above (C2-H1...O2 ($x, y+1, z$), still shown with red dotted lines) also help to form the 2D plane. The right half is illustrated by the simplified structures. (d) Three-dimensional structure formed by the aforementioned three kinds of intermolecular C-H...O H-bonds, view along the b axis. The sloping chain extending along the c axis is formed by the second kind of H-bonds. Only three layers are present and their adjacent layers have been

omitted for clarity.

Similar as that in dimer **1**, no valuable π - π stacking interactions were found and only hydrogen bonding occurs in the packing structure of **2**. The geometries of hydrogen bonds are listed in **Table S2** and the schematic illustrations are shown in **Fig. 2**. As can be seen, there are three kinds of intermolecular C–H \cdots O hydrogen bonds in **2**. The first (C2–H1 \cdots O2^(x, y+1, z)) and the second (C5–H4 \cdots O1^(-x, -y+1, -z)) kinds of H bonds link **2** into two kinds of 1D chains with different orientations (along *b* and *c* axis respectively) (**Fig. 2(b)**). The third kind of H bonds (C3–H2 \cdots O2^(-x+0.5, y+0.5, -z+1.5)) link **2** into a 2D layer framework (**Fig. 2(c)**). Packing of these layers in the crystal is stabilized by the second kind of H bonds (**Fig. 2(d)**).

3. 1. 3. Crystal structure of **3**

Compound **3** is the result of hydrolysis of dimer **2** and crystallizes in two forms, one has a water molecule (**3-1**) and another one has none (**3-2**). Das and Dastidar have synthesized this compound in 2013 but failed to grow X-ray quality single crystals despite serious efforts. [29]

X-ray structural analysis reveals that the asymmetric unit of **3-1** comprises of six monoprotonated maleate anions (**MMA**), three protonated propylenediammonium dications (**PPD**) and one H₂O molecule (**Fig. 3(a)**), while **3-2** contains four **MMA** and two **PPD** (**Fig. 3(c)**).

The two C–O distances bonded to the same C in **MMA** are obviously different (**Table S3**). In **3-1**, the C–O bonds lie in the ranges of 1.214(2) – 1.245(2) Å and 1.262(3) – 1.289(3) Å, respectively. In **3-2**, the ranges are 1.173(7) – 1.245(7) Å and 1.253(7) – 1.352(8) Å, respectively. This proves the incomplete deprotonation of the maleic acid. Similar to what we have calculated in our previous paper, [30] hydrogen transfer from maleic acid to propylenediamine was carried out after the hydrolysis of dimer **2**, yielding three oppositely charged spheres. Our DFT calculations (B3LYP/6-311+G(d,p)) prove that the proton transfer is inevitable in implicit solvent model of CPCM, *i.e.* no stable structure including neutral fragments can be obtained in ethanol solution. Maleic acid and propylenediamine can coexist only in gas phase, with around 149.5 kJ/mol higher energy than that of ionic fragments (two **DMA** and one **PPD**, calculated at DFT/B3LYP/6-311+g(d,p) level), and the former will always be optimized into the latter in ethanol solution. These ionic fragments were held together by electrostatic interactions as well as hydrogen bonds (**Tables S4-S5**). The two protons act as a “glue” to hold the diammonium cations and various anions together. The **MMA** structures in **3-1** and **3-2** are nearly the same except some differences in the intra-molecular hydrogen bond. Most **MMA** have linear O–H \cdots O intra-molecular hydrogen bonds, forming pseudo seven-membered rings, thus locking the molecular conformation and eliminating conformational flexibility. But three **MMA** in **3-2** have not formed this kind of intra-molecular hydrogen bonds, because these hydrogen atoms of –OH groups were placed in geometrically calculated positions and refined using AFIX 147 constraints available in SHELXL97, instead of being experimentally determined in electron density maps as did in most other **MMA**.

Unlike the *g-g* conformation adopted by dimer **1** and dimer **2**, the **PPD** dimers in **3-2** all employ *gauche-anti* conformation (abbreviated as *g-a*). More interestingly, two different conformations of **PPD** are present in **3-1**, *i.e.* *g-a* and *a-a* (denotes anti–anti conformation). This pattern, that is, coexistence of *g-a* and *a-a*, has hardly been observed experimentally in the solid state. [31] As we know, the flexibility of the C3 bridged dimers can exhibit three popular conformations: *a-a*, *g-a* and *g-g*. Then what's the difference between them in energy? Which one is the most stable, energetically favorable conformation of the molecule? Having in mind that the degree of freedom of molecules in solution state remains free, there is an immediate possibility that molecule may adopt any kinds of stable conformation. However, in

solid state, does molecule exist in one stable conformation or the most stable conformation? These uncertainties promote us to explore all possible conformations of PPD through relaxed PES scans over its full range (see **5. Relaxed potential energy surface scans**).

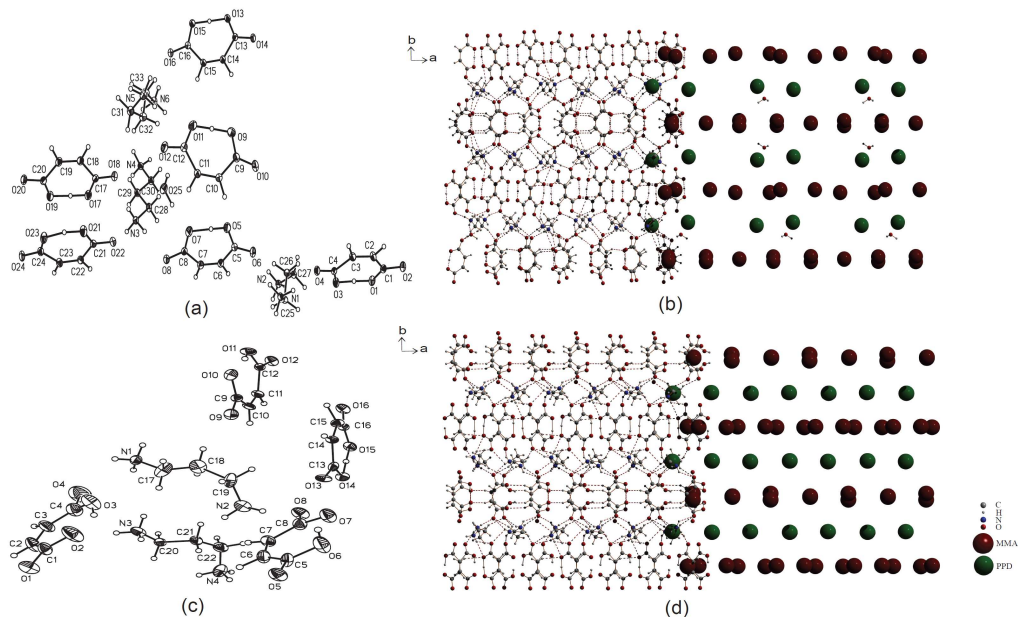


Fig. 3. (a) Atom numbered molecular structure of **3-1** with displacement ellipsoids for non-H atoms drawn at the 30% probability level at 298 K. (b) Projection of layers of **MMA** alternating with layers of **PPD** onto the *ab* plane in the crystal of **3-1**. In the right half, dicationic and anionic backbones are shown with color balls that lie in their center of gravity. Red ones present **MMA** and green ones present **PPD**. (c) Atom numbered molecular structure of **3-2** with displacement ellipsoids for non-H atoms drawn at the 30% probability level at 298 K. (d) Perspective view of the structure of **3-2** in the *ab* plane in aforementioned styles.

Supramolecular structures of **3-1** and **3-2** show similar alternating layers of **MMA** and **PPD**, which are parallel to the *ac* plane (**Fig. 3(b)(d)**). In the crystal structure of **3-1**, each **PPD** was attached with eight neighboring **MMA** and each **MMA** was attached with four neighboring **PPD** via N–H···O and C–H···O interactions. The solvate water molecules were occluded via O–H···O (O25—H55···O7 and O25—H56···O10 ($x, -y+1/2, z+1/2$)) and N–H···O (N4—H41···O25 ($x, y, z+1$)) interactions within the interstitial space of one **PPD** and two **MMA**. Though there is no water molecules in the crystal structure of **3-2**, **PPD** and **MMA** were involved in charge-assisted hydrogen bonding with each other similar as that in **3-1**. All of them self-assembled into a 3D hydrogen-bonding ionic network. In one word, the overall hydrogen-bonding ionic network may be described as regular alternating layers of deprotonated acid moieties (**MMA**) pillared by diammonium cations (**PPD**) sustained by electrostatic attractions and various hydrogen bonds.

4. Searching and analyzing in Cambridge Structural Database (CSD)

Careful analyses of the foregoing discussions on single crystal structures revealed interesting observations. In the process of hydrolytic degradation, the conformations of three propylene linking dimers change from g-g to g-a and a-a. This series of dimers containing 'propylene linkers' were designed with the assumption that progressive reaction should impart an influence in the conformations though the flexible trimethylene may adjust itself according to the non-covalent interactions between the bulky headgroups. Their single crystal structures show that no product retains initial g-g conformations at the end of the reaction process. But this phenomenon does not prove that

1,3-diammonium propane (i.e. **PPD**) cannot adopt g-g conformations. A CSD [15] search revealed 24 crystals that contain **PPD** fragment having g-g conformations among 258 entries with established **PPD** conformations (**Table S6**, some crystals with disorder or uncertainty are not included). By the way, there are 80 crystals acting as g-a conformation (**Table S7**) and 154 crystals acting as a-a conformation (**Table S8**). Obviously, a-a conformation may be the most stable one. Then, why g-g and g-a conformations can also become the preferences in some crystals?

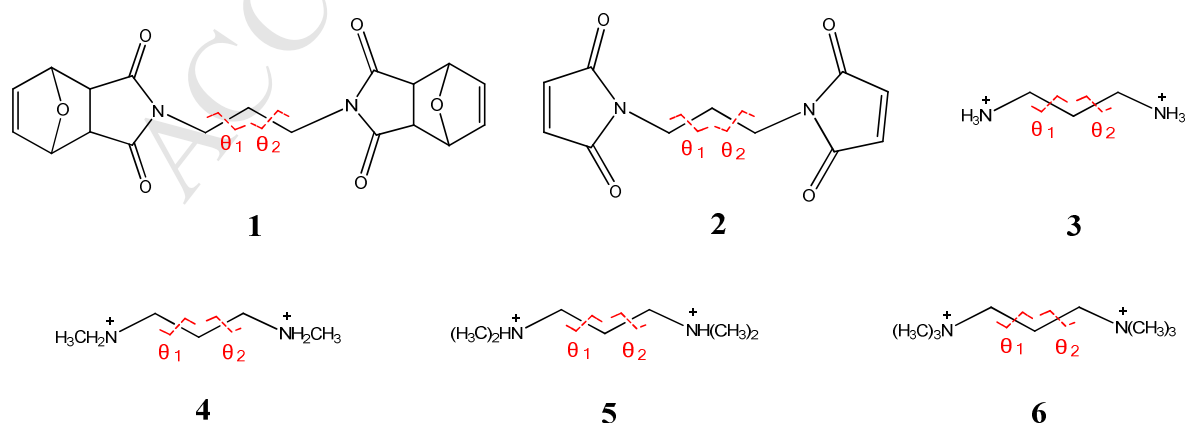
An extended CSD survey was conducted to obtain more information about the trimethylene conformation. It should be noted that only symmetrical N-substituted trimethylenediammonium / trimethylenediamine dimers are counted, because asymmetrical models will introduce more complicated interactions and provoke different responses for the two rotating C-C bonds. Besides dimers, most multimers / polymers are counted if they have definite conformations. At last, the total amount of 658 entries was investigated. If the aforementioned 154 crystals having **PPD** were excluded, 504 entries having at least one non-hydrogen moieties at their termini were retained. We found 125 g-g conformations (**Table S9**), 190 g-a conformations (**Table S10**) and 189 a-a conformations (**Table S11**) in 504 crystal structures. This is a different type of results, and we cannot expect that one or two conformations are overwhelmingly stable as it does in **PPD** conformations. That is to say, these three popular conformations (a-a, g-a and g-g) may have similar stabilities, especially when there exist different kinds of weak interactions. Then, how about the energy barriers between different conformations?

5. Relaxed potential energy surface scans

There are two ways to study conformational stability. One includes statistical analysis of large datasets of diversified architectures. The other way of studying significant conformational changes is through computationally addressing the energy changes upon rotating the most popular single bonds.

It remains yet to understand how many of the energetically accessible minima of propylene linking dimers and the relative energies/energy barriers among them can be observed. To gain further insight, relaxed potential energy scans were carried out along the two flexible coordinates (θ_1 and θ_2) governing the position and orientation of two terminal groups (**Scheme 2**).

Except aforementioned three dimers (**1**, **2**; for clarity, **3** denotes **PPD** in this section), a series of three N-methyl substituted propylenediammonium dications from CSD were also discussed for comparison. They are abbreviated as **4**, **5** and **6** (**Scheme 2**). The computational methods used in this study have been described in detail in “2.4 Computational Study”.



Scheme 2. Six dimers were investigated for various conformations through full range relaxed PES scans of two dihedral angles (θ_1 and θ_2). The number of dihedral angles was labeled according to the atom number of N, which ensures the consistency in all calculations.

The relaxed PES maps are shown in **Figs. S7-S14** and the corresponding data (relative energies and dihedrals) are listed in **Tables S12-S19**. **Figs. S9** and **S11** as well as **Tables S14** and **S16** are the results calculated in 6-31+G* basis set for comparison with that of 3-21G* basis set. As we can see, the more complicated the dimer, the more number of minima and energy levels on the map. For example, **1** has 20 minima and 20 energy levels (from A to T), **2** has 17 minima and 13 energy levels (from A to M), while **3** has only 14 minima and 5 energy levels (from A to E). **4**, **5** and **6** have 13, 12, 10 minima, 10, 9 and 6 energy levels, respectively, mainly depends on the degree of coupling between terminals. As we mentioned above, the minima on the PES map don't correspond precisely to the local stable conformation. So all minima have been re-optimized using larger basis set 6-311+G(d,p) (both in gas phase and ethanol solutions). The relative energies and dihedral angles (θ_1 and θ_2) upon re-optimization are also listed in **Tables S12, S13, S15, S17-S19** along with the results extracted from PES scans. As can be seen, some different "stable" rotamers on the PES map were optimized into the same one. As a result, only 7 g-g rotamers, 3 g-a rotamers and 1 a-a rotamer remained in dimer **1** after re-optimization in larger basis set 6-311+G(d,p) in gas phase (the overall energy order follows g-a < g-g < a-a), and 5 g-g, 3 g-a, 1 a-a rotamers remained after re-optimization in 6-311+G(d,p) in ethanol solution (the overall energy order follows a-a < g-a < g-g). The relative energy gaps between different stable minima reduced from the highest 70.61 kJ/mol in PES to 22.78 kJ/mol in 6-311+G(d,p)-gas and 14.00 kJ/mol in 6-311+G(d,p)-solution. Dimer **2** has similar results. Only 3 g-g, 1 g-a and 1 a-a rotamers were left after re-optimization in gas phase (the overall energy order follows g-a < g-g < a-a), while 1 g-g, 1 g-a and 1 a-a rotamers were left after re-optimization in ethanol solution (the energy order follows a-a < g-a < g-g). The relative energy gaps between different stable minima increased a little from the highest 13.02 kJ/mol in PES to 13.92 kJ/mol in 6-311+G(d,p)-gas and reduced dramatically to 6.72 kJ/mol in 6-311+G(d,p)-solution. Commonly, a-a conformations are a little more stable than experimentally obtained g-g conformations, which is probably due to the presence of hydrogen bonds that are not taken into account in calculations. Another probability is that we just get one of the stable rotamers (having non-statistical significance) and other rotamers may also appear when many more crystal structures are determined. That's the case for dimers **3** to **6**.

From dimer **3** to dimer **6**, the numbers of stable rotamers are the same after re-optimization in 6-311+G(d,p)-gas and 6-311+G(d,p)-solution, but all less than that in PES maps. Only 1 g-g, 1 g-a and 1 a-a rotamers remained for dimer **3** and the energy order follows a-a < g-a < g-g. For dimer **4**, there remained 1 g-g, 2 g-a and 3 a-a rotamers and the overall energy order follows a-a < g-a < g-g. For dimer **5**, there remained 1 g-a and 2 a-a rotamers and the overall energy order follows a-a < g-a. Only 1 a-a rotamer remained for dimer **6**. All energy gaps between different minima are dramatically reduced in solution. The highest ones are 9.17, 13.75 and 5.76 kJ/mol for dimers **3**, **4**, **5** respectively. Energy gap is meaningless for dimer **6** because only one stable minimum was left. Interestingly, the match-up between experiment (conformations in crystal structures indicated by a CSD survey, see reference [32]) and calculation is surprisingly good. That is to say, all kinds of conformations can be found for dimers **3** and **4**, but only a-a conformations can be found for dimer **6**. While dimer **5** is somewhat different from our calculation because there is one crystal (CSD refcode MOWGIP) having g-g conformation. This difference is important in evaluating strong and weak intermolecular interactions for two reasons. First, in the X-ray crystal structure there exist strong hydrogen bonds involving cationic donors and anionic

acceptors ($N^+-H\cdots SCN^-$) [9] that were not considered in theoretical study. Second, in the optimized geometry of the dimer, only one dication ion was considered and no counter anions appeared. The variation of the electrostatic attraction that could exist between two ions is not taken into account in the calculation. Nevertheless, the calculated results focus on the conformations of the propylene linker itself, without any bias for certain conformations. These results may help to find and investigate various non-covalent interactions.

As a convenient choice for this investigation, we concentrated on the relative energies of the stable minima and the energy barriers separating them. In order to draw a visual landscape of these energies, we have transferred the 3D PES maps to 2D lines focusing on energy gap and energy barrier (**Fig. 4(c)**). The results are summarized in **Fig. 4**, all calculated at the DFT/B3LYP/6-311+g(d,p) level in ethanol solution.

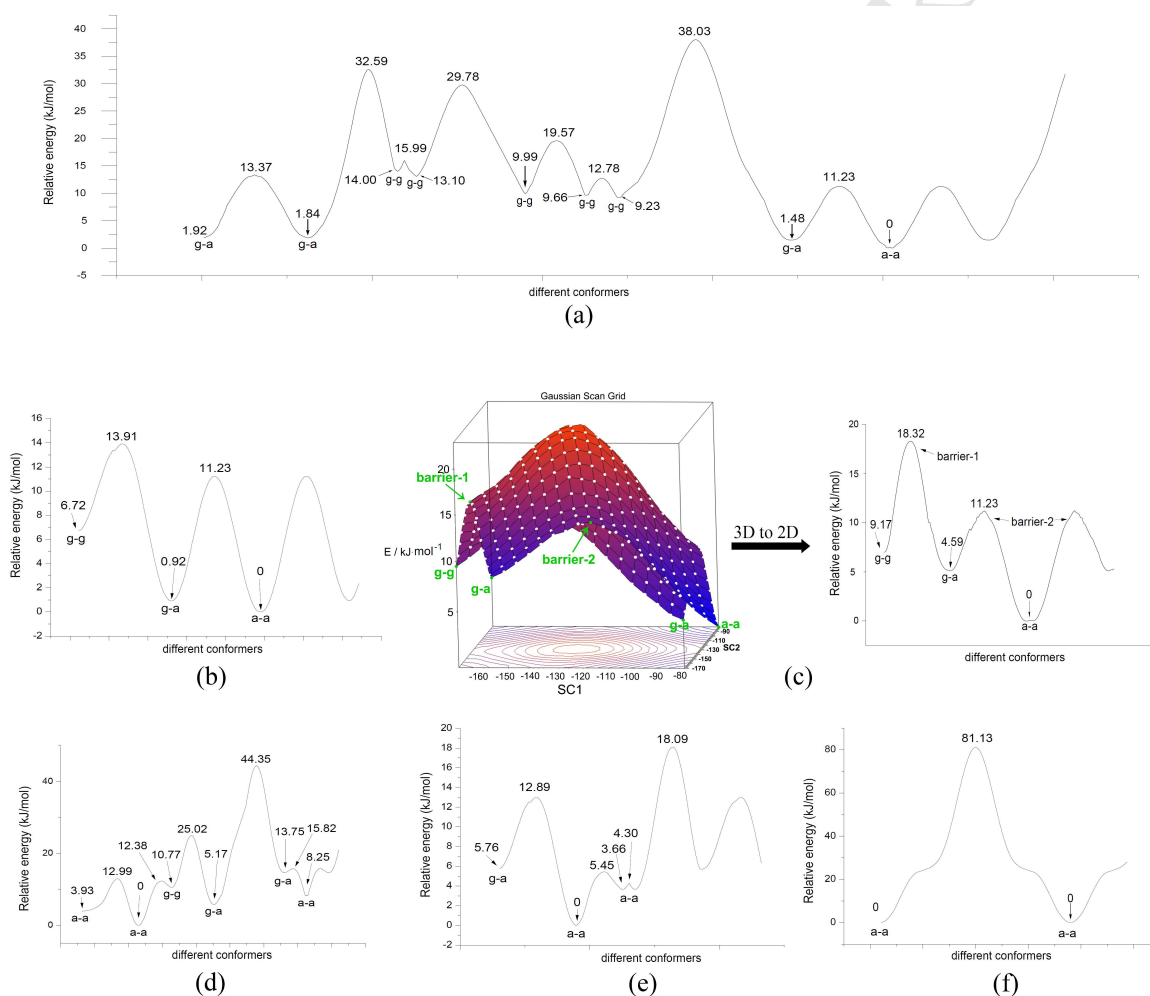


Fig. 4. The relative energies of the stable minima and the energy barriers separating them for different dimers, all calculated at the DFT/B3LYP/6-311+g(d,p) level in ethanol solution. (a) dimer 1; (b) dimer 2; (c) dimer 3, this picture shows the method of changing 3D PES maps into 2D lines, where the key point lies in the energy barriers; (d) dimer 4; (e) dimer 5; (f) dimer 6.

For dimer 1, the theoretical calculations suggest that a-a rotamer is the most stable conformation, and g-a conformations have little difference in energy with a-a (the difference is only about 1.48-1.92 kJ/mol). The finally obtained conformation is in g-g, which is collectively determined by weak interactions (hydrogen bonds, see **Table S1**) and the energy barriers. As shown in **Fig. 4(a)**, g-g

conformations can be trapped in local conformational minima with 9.23-14.0 kJ/mol above the global minimum. The energy barriers are about 32.59-38.03 kJ/mol, which cannot be overcome very easily, further supports the probability that molecule may adopt one local stable conformation, regardless the ranking in energy sequence. For dimers **2**, **3** and **5**, the energy barrier is no more than 20 kJ/mol, which means that the final conformation has more trends to seek the most stable one. A likely explanation for the differences between the calculated and the observed rotational conformation could be hydrogen bonding and other intermolecular interactions. For dimer **4**, the less stable g-g conformation is very readily to change into a-a rotamer. The one example of g-g conformation may be ascribed to three kinds of N-H...O hydrogen bonds. [33] For dimer **6**, the a-a rotamer is so stable and there is no energy barrier for other conformations to evolve into a-a conformation. So it is reasonable to predict that conformations other than a-a will never be found in the future.

In conclusion, the final conformation is jointly determined by relative energy of different rotamers and energy barriers separating them, the former can be influenced by various weak interactions. At last, the randomness may play a role under certain conditions. After all, seldom structure can be unambiguously predicted as that in dimer **6**.

6. Conclusions

Four single-crystal structures related with the same reaction have been investigated. All have propylene linked dimers but the trimethylene linking chains have different conformations. **1** and **2** are in g-g conformation, while **3-1** and **3-2** are in g-a and a-a conformations (only without g-g conformation). Provoked by these phenomena, we performed statistical analysis of large datasets of CSD crystal data. For protonated propylenediammonium dication (**PPD**), a-a conformations are an absolute majority (154 in 258 entries) and g-g conformations are very few (24 in 258 entries). But for other symmetrical 'propylene linker' diammonium/diamine dimers containing at least one non-hydrogen terminal groups, the number of g-g and g-a conformations have not so much difference (125 g-g and 189 a-a in 504 entries). It seems that these three popular conformations have similar stability on the point that "nature always seeks stability".

In order to draw a probable landscape of the energy changes among different stable conformations of propylene linked dimers, six model structures were chosen to draw full range 2D PES maps. The fully relaxed PES scan using small basis functions (DFT/B3LYP/3-21G*) combined with local minima re-optimizing with more sophisticated basis functions (DFT/B3LYP/6-311+G(d,p), in gas and solution) represent a less time-consuming and more reliable approach to the determination of conformational stability of propanediyl bridging chains. Energy barriers were got through relaxed one-dimensional or two-dimensional PES scans between two stable conformers. Inspection of calculated results show that most energy gaps between different stable conformations are no more than 15 kJ/mol, and most energy barriers separating them are no more than 40 kJ/mol. Although the calculations were performed with a specific step size and many non-covalent interactions are not taken into account, the results can still be used to predict the number of relatively stable rotamers, evaluate the relative stability of different conformations, understand the role of randomness in the formation of the final structure, help to find and investigate various non-covalent interactions when compared with observed results.

7. Acknowledgments

The authors are thankful to the Science & Technology Development Projects of Shandong Province in China (No. 2011GGX10706 and 2012GGX10702) and the National Natural Science Foundation of PR China (NSFC, No. 21103100) for financial support. Generous support in computing resources from

the National Supercomputer Center in Jinan, China, is greatly appreciated.

Supplementary Material

Supplementary Information available: **Tables S1 – S19, Figures S1 – S14** mentioned in the text. Crystallographic information files of five compounds. CCDC < 1446299, 1519779, 1519777 and 1519778 > contains the supplementary crystallographic data for < **1**, **2**, **3-1** and **3-2** >. These data can be obtained free of charge from The Cambridge Crystallographic Data Centre via http://www.ccdc.cam.ac.uk/data_request/cif, or from the Cambridge Crystallographic Data Centre, 12 Union Road, Cambridge CB2 1EZ, UK; fax: (+44) 1223-336-033; or e-mail: deposit@ccdc.cam.ac.uk.

References and notes

- [1] P.S. Portoghese, *J. Med. Chem.* 35 (1992) 1927-1937.
- [2] (a) G. Berube, *Current Medicinal Chemistry*, 13 (2006) 131-154;
 (b) T.A. Hill, S.G. Stewart, S.P. Ackland, J. Gilbert, B. Sauer, J. A. Sakoff and A. McCluskey. *Bioorg. Med. Chem.* 15(2007) 6126-6134;
 (c) S. S. Cheng, Y. Shi, X. N. Ma, D. X. Xing, L. D. Liu, Y. Liu, Y. X. Zhao, Q. C. Sui, X. J. Tan, *J. Mol. Struct.* 1115 (2016) 228-240.
- [3] (a) D.A. Fowler, J.L. Atwood, G.A. Baker, *Chem. Commun.* 49 (2013) 1802-1804;
 (b) D. Bagnis, L. Beverina, H. Huang, F. Silvestri, Y. Yao, H. Yan, G. A. Pagani, T. J. Marks, A. Facchetti, *J. Am. Chem. Soc.* 132 (2010) 4074–4075;
 (c) R. Boese, H. C. Weiss, D. Bläser, *Angew. Chem., Int. Ed.* 38 (1999) 988–992;
 (d) L. Ding, H. Li, T. Lei, H. Ying, R. Wang, Y. Zhou, Z. Su, J. Pei, *Chem. Mater.* 24 (2012) 1944-1949;
 (e) K. Avasthi, S.M. Farooq, R. Raghunandan, P.R. Maulik, *J. Mol. Struct.* 927 (2009) 27-36.
- [4] K. Avasthi, D.S. Rawat, P.R. Maulik, S. Sarkhel, C.K. Broder, J.A.K. Howard, *Tetrahedron Lett.* 42 (2001) 7115-7117.
- [5] (a) G. Mukherjee, K. Biradha, *Cryst. Growth Des.* 11(2011) 924–929;
 (b) G. Mukherjee, K. Biradha, *Cryst. Growth Des.* 13(2013) 4100-4109.
- [6] (a) D.T. Browne, J. Eisinger, N.J. Leonard, *J. Am. Chem. Soc.* 90 (1968) 7302–7323;
 (b) L.S. Rosen, A. Hybl, *Acta Crystallogr. B* 27 (1971) 952-960;
 (c) H. Kagechika, I. Azumaya, A. Tanatani, K. Yamaguchi, K. Shudo, *Tetrahedron Lett.* 40 (1999) 3423-3426;
 (d) Y. Kajikawa, N. Azuma, K. Tajima, *Inorg. Chim. Acta*, 288 (1999) 90-100;
 (e) J. Zhao, L. Yang, K. Ge, Q. Chen, Y. Zhuang, C. Cao, Y. Shi, *Inorg. Chem. Comm.* 20 (2012) 326-329;
- [7] (a) N.J. Leonard, *Acc. Chem. Res.* 12 (1979) 423–429;
 (b) L.F. Newcomb, S.H. Gellman, *J. Am. Chem. Soc.* 116(1994) 4993–4994;
 (c) K. Avasthi, D.S. Rawat, T. Chandra, D.S. Bhakuni, *Indian J. Chem.* B37 (1998) 754–759;
 (d) P.R. Maulik, K. Avasthi, G. Biswas, S. Biswas, D.S. Rawat, S. Sarkhel, T. Chandra, D.S. Bhakuni, *Acta Crystallogr. C* 54 (1998) 275–277;
 (e) Y.P. Pang, J.L. Miller, P.A. Kollman, *J. Am. Chem. Soc.* 121 (1999) 1717–1725;
 (f) P.R. Maulik, K. Avasthi, S. Sarkhel, T. Chandra, D.S. Rawat, B. Logsdon, R.A. Jacobson, *Acta Cryst. C* 56 (2000)

- 1361-1363;
- (g) K. Avasthi, S. Aswal, P.R. Maulik, *Acta Cryst. C* 57 (2001) 1324-1325;
- (h) H. Hao, F. Liu, H. Su, Z. Wang, D. Wang, R. Huang and L. Zheng, *CrystEngComm*, 14 (2012) 6726-6731;
- (i) P.P. Sun, Q. Chen, X. Zhu, B.L. Li, H.Y. Li, *Polyhedron* 52 (2013) 1009–1015;
- (j) J.T. Shi, K.F. Yue, B. Liu, C.S. Zhou, Y.L. Liu, Z.G. Fang, Y.Y. Wang, *CrystEngComm*, 16 (2014) 3097-3102.
- [8] A. García-Raso, F.M. Albertí, J.J. Fiol, A. Tasada, M. Barcelo-Oliver, E. Molins, C. Estarellas, A. Frontera, D. Quinónero, and P.M. Deya, *Cryst. Growth Des.* 9 (2009), 2363-2376.
- [9] D.J. Wolstenholme, J.J. Weigand, E.M. Cameron, T.S. Cameron, *Cryst. Growth Des.* 9 (2009) 282-290.
- [10] J. R. Carney, T. S. Zwier, *Chem. Phys. Lett.* 341 (2001), 77–85.
- [11] (a) D. Brawn and A. Ceulemans, *J. Phys. Chem.* 99 (1995) 11101-11114;
- (b) C.W. Bauschlicher, *Chem. Phys. Lett.* 246 (1995) 40-44.
- [12] A.D. Becke, *J. Chem. Phys.* 98 (1993) 5648-5652.
- [13] P.J. Stevens, F.J. Devlin, C.F. Chablowski and M.J. Frisch, *J. Phys. Chem.* 98 (1994) 11623-11627.
- [14] C.W. Bauschlicher Jr. and H. Partridge, *J. Chem. Phys.* 103 (1995) 1788-1791.
- [15] (a) F. H. Allen, *Acta Crystallogr., Sect. B: Struct. Sci.* 58 (2002) 380-388;
- (b) Cambridge Structure Database search, CSD Version 5.36, updated on May, 2015.
- [16] (a) S. Baggio, A. Barriola and P.K. de Perazzo, *J. Chem. Soc. Perkin Trans. 2* (1972) 934-937;
- (b) B.M. Ramirez, G.D. de Delgado, W.O. Velasquez, G.M. Perdomo, *Z. Kristallogr.-New Crystal Structures*, 213 (1998) 197-198;
- (c) Y.W. Goh, B.R. Pool, J.M. White, *J. Org. Chem.* 73 (2008) 151-156;
- [17] Y. Musa and M.P. Stevens, *J. Poly. Sci.: Part A-1*, 10 (1972) 319-327.
- [18] G. M. Sheldrick, *SADABS*, Bruker AXS Inc., Madison, Wisconsin, USA, 2004.
- [19] G. M. Sheldrick, *Acta Crystallogr, Sect. A*, 64 (2008) 112-122.
- [20] Bruker APEX II (version 2.0-1), SAINT (version 7.23A), XPREP (version 2005/2), SHELXTL (version 6.1). Bruker AXS Inc., Madison, Wisconsin, USA, 2005.
- [21] K. Brandenburg, H. Putz, *DIAMOND*. Crystal Impact GbR, Bonn, Germany, 2005.
- [22] (a) J. P. Perdew, J. A. Chevary, S. H. Vosko, K. A. Jackson, M. R. Pederson, D. J. Singh, C. Fiolhais, *Phys. Rev. B* 46 (1992) 6671-6687;
- (b) Y. Wang, J. P. Perdew, *Phys. Rev. B* 44 (1991) 13298-13307;
- (c) A.D. Becke, *Phys. Rev. A* 38 (1988), 3098-3100;
- (d) C. Lee, W. Yang, R.G. Parr, *Phys. Rev. B: Condens. Matter Mater. Phys.* 37 (1988) 785-789.
- [23] W. J. Hehre, L. Radom, P. V. R. Schleyer, J. A. Pople, *Ab Initio Molecular Orbital Theory*; Wiley: New York, 1986.
- [24] (a) V. Barone and M. Cossi, *J. Phys. Chem. A* 102 (1998) 1995-2001;
- (b) M. Cossi and V. Barone, *J. Chem. Phys.* 115 (2001) 4708-4717;
- (c) M. Cossi, N. Rega, G. Scalmani and V. Barone, *J. Comput. Chem.* 24 (2003) 669-681.

- [25] M. J. Frisch, G. W. Trucks, H. B. Schlegel, G. E. Scuseria, M. A. Robb, J. R. Cheeseman, J. A. Jr. Montgomery, T. Vreven, K. N. Kudin, J. C. Burant, J. M. Millam, S. S. Iyengar, J. Tomasi, V. Barone, B. Mennucci, M. Cossi, G. Scalmani, N. Rega, G. A. Petersson, H. Nakatsuji, M. Hada, M. Ehara, K. Toyota, R. Fukuda, J. Hasegawa, M. Ishida, T. Nakajima, Y. Honda, O. Kitao, H. Nakai, M. Klene, X. Li, J. E. Knox, H. P. Hratchian, J. B. Cross, V. Bakken, C. Adamo, J. Jaramillo, R. Gomperts, R. E. Stratmann, O. Yazyev, A. J. Austin, R. Cammi, C. Pomelli, J. W. Ochterski, P. Y. Ayala, K. Morokuma, G. A. Voth, P. Salvador, J. J. Dannenberg, V. G. Zakrzewski, S. Dapprich, A. D. Daniels, M. C. Strain, O. Farkas, D. K. Malick, A. D. Rabuck, K. Raghavachari, J. B. Foresman, J. V. Ortiz, Q. Cui, A. G. Baboul, S. Clifford, J. Cioslowski, B. B. Stefanov, G. Liu, A. Liashenko, P. Piskorz, I. Komaromi, R. L. Martin, D. J. Fox, T. Keith, M. A. Al-Laham, C. Y. Peng, A. Nanayakkara, M. Challacombe, P. M. W. Gill, B. Johnson, W. Chen, M. W. Wong, C. Gonzalez, J. A. Pople, Gaussian 03, revision C.02; Gaussian, Inc.: Wallingford, CT, **2004**.
- [26] (a) T. Nakatani, K. Jinpo & N. Noda, *Chem. Pharm. Bull.* 55(1) (2007) 92–94;
 (b) V. Rao, S. Navath, M. Kottur, J.R. McElhanon, D.V. McGrath, *Tetrahedron Lett.* 54 (2013) 5011-5013.
- [27] (a) M. W. Lee & W. C. Herndon, *J. Org. Chem.* 43 (1978) 518-518;
 (b) P.X. Iten, A.A. Hofmann & C.H. Eugster, *Helv. Chim. Acta* 62 (1979) 2202-2210; and litt. therein.
- [28] (a) J.L. Feng, C.Y. Yue, K.S. Chian, *e-Polymers*, 6(1) (2006) 566–579;
 (b) J.L. Feng, C.Y. Yue, K.S. Chian, *e-Polymers*, 6(1) (2006) 633–643;
 (c) C.E. Hoyle, S.C. Clark, K. Viswanathan and S. Jonsson, *Photochem. Photobiol. Sci.*, 2 (2003) 1074–1079;
 (d) I. Franke, A. Pingoud, *J. Protein Chem.* 18(1) (1999) 137-146;
 (e) K. Belina, *J. Therm. Anal.* 50(4) (1997) 655-663;
 (f) J.C. Cheronis, E.T. Whalley, K.T. Nguyen, S.R. Eubanks, L.G. Allen.; M.J. Duggan, S.D. Loy, K.A. Bonham, J.K. Blodgett, *J. Med. Chem.* 35(9) (1992) 1563-1572;
 (g) M. Baksay, K. Belina, F. Biro, J. Varga, *Periodica Polytechnica, Chemical Engineering*, 33(1) (1989) 21-27;
 (h) J. Put and F.C. De Schryver, *J. Am. Chem. Soc.* 95(1) (1973) 137-145;
 (i) W.J. Feast, J. Put, F.C. De Schryver, F.C. Compennolle, *Organic Mass Spectrometry*, 3(4) (1970) 507-517.
- [29] U.K. Das, P. Dastidar, *Cryst. Growth Des.* 13 (10) (2013) 4559-4570.
- [30] X.J. Tan, S.S. Cheng, Y. Shi, D.X. Xing, Y. Liu, H. Li, W.Q. Feng, J.B. Yang, *J. Mol. Struct.* 1125 (2016) 514-521.
- [31] A CSD (CSD version 5.36, updated on May, 2015) search revealed that such a pattern only appeared in 13 crystal structures. The following are their entry ID. Coexistence of g-a & a-a: HUBQIG, HUBQOM, LASNUQ, DIHYUP, TICDEQ, EKAWIX, XEHLED and YUZGAC; Coexistence of g-a & g-g: SOYTIL, SOZGUL, TIBCOY and GIWPIN; Coexistence of g-g & a-a: OHEGAJ.
- [32] Sum up the CSD survey results listed from **Table S6** to **Table S11**, there are 154 a-a, 80 g-a, 24 g-g conformations among 258 structures containing dimer **3**, the refcodes are listed in **Table S6-S8**; there are 2 a-a (refcodes: YICTEJ and TOWLEY), 2 g-a (refcodes: XELPIO and EZAYOT), 1 g-g (refcode: UTUNAZ) conformations among 5 structures containing dimer **4**; there are 6 a-a (refcodes: FIRKEW, RACNUE, SUKZAZ, GUGXIR, TIQFIJ, and LANNIY), 2 g-a (refcodes: MOJDOE and MABCEZ), 1 g-g (refcode: MOWGIP) conformations among 9 structures

containing dimer **5**; there are 5 a-a (refcodes: HMPAGI, TIBRIF, TIDVOR, TIDVUX and ZUCYED), no g-a and g-g conformations among 5 structures containing dimer **6**.

[33] G. Wang, P. Wang, Z. Li, H. Huang, Y. Wang, J. Lin, *Solid State Sciences*, 13(2011) 1567-1572.

Keywords: propylene linker, dimer, crystal structure, conformation, 2D fully relaxed potential-energy surface.

ACCEPTED MANUSCRIPT

Highlights

- 1) Four single-crystal structures have been investigated; molecular conformations and weak interactions have been analyzed.
- 2) Statistical analysis of CSD database revealed that a-a, g-a and g-g conformations may have similar stability for most N-substituted symmetrical 'propylene linker' diammonium/diamine dimmers.
- 3) Full range two-dimensional fully relaxed potential-energy surfaces scans of six 'propylene linker' dimers were calculated in order to probe the conformations of the propylene linker itself. This study provides a better understanding of the role that some factors can play in the formation of the final conformations.
- 4) Our method represents a less time-consuming and more reliable approach to the determination of conformational stability of propanediyl bridging chains.